PCCP

PAPER

View Article Online
View Journal | View Issue

Cite this: *Phys. Chem. Chem. Phys.*, 2014, **16**, 14669

A new ultrafast superionic Li-conductor: ion dynamics in $Li_{11}Si_2PS_{12}$ and comparison with other tetragonal LGPS-type electrolytes†

Alexander Kuhn,[a] Oliver Gerbig,[a] Changbao Zhu,[a] Frank Falkenberg,[a] Joachim Maier[a] and Bettina V. Lotsch*[abc]

Received 11th May 2014,
Accepted 30th May 2014

DOI: 10.1039/c4cp02046d

www.rsc.org/pccp

We report on a new ultrafast solid electrolyte of the composition $Li_{11}Si_2PS_{12}$, which exhibits a higher room-temperature Li ion diffusivity than the present record holder $Li_{10}GeP_2S_{12}$. We discuss the high-pressure synthesis and ion dynamics of tetragonal $Li_{11}Si_2PS_{12}$, and comparison is made with our investigations of related members of the LMePS family, *i.e.* electrolytes of the general formula $Li_{11-x}Me_{2-x}P_{1+x}S_{12}$ with Me = Ge, Sn : $Li_{10}GeP_2S_{12}$, Li_7GePS_8, $Li_{10}SnP_2S_{12}$. The structure and dynamics were studied with multiple complementary techniques and the macroscopic diffusion could be traced back to fast Li ion hopping in the crystalline lattice. A clear correlation between the diffusivity and the unit cell volume of the LGPS-type electrolytes was observed.

In 2011, the new solid lithium electrolyte $Li_{10}GeP_2S_{12}$ (LGPS) was reported, featuring liquid-like Li ion conduction in a crystalline solid matrix.[1,2] The ultrafast room temperature transport of tetragonal LGPS with a conductivity of several mS cm^{-1} came as a surprise as it exceeds the values of the best crystalline Li conductors by one order of magnitude. Therefore, there has been a strong upsurge of interest recently in realizing LGPS-type materials based on the homologous elements Si and Sn. A theoretical study published by Ceder and coworkers highlights the potential of such hypothetical tetragonal LGPS-type Li ion conductors.[3] $Li_{10}SnP_2S_{12}$ was recently reported[4,5] and showed slightly reduced Li mobility as compared to LGPS, in line with the predictions by Ceder *et al.*

Here, we (i) report the successful high-pressure synthesis of the Si-analogue, $Li_{11}Si_2PS_{12}$, and (ii) present a comparative fundamental study of the Li ion dynamics in the four LGPS-type electrolytes reported so far, $Li_{11}Si_2PS_{12}$ (LSiPS, this study), $Li_{10}SnP_2S_{12}$ (LSnPS, this study and ref. 4 and 5), $Li_{10}GeP_2S_{12}$ (ref. 1 and 6) and Li_7GePS_8 (ref. 6). LSnPS and LSiPS were comprehensively characterized both with respect to their structure and Li ion dynamics and compared with the results previously published on LGPS.[6] In excellent agreement with the theoretical predictions in ref. 3, LSiPS shows an even higher Li diffusivity than LGPS while LSnPS has a slightly lower Li diffusivity. A clear correlation between the diffusivity and the unit cell volume was observed.

Tetragonal $Li_{10}SnP_2S_{12}$ was prepared by heating elemental Sn, P, S, and Li_2S to 653 K for 10 h with an additional sintering step at 723 K for two days, *cf.* ref. 4 and 5. The tendency of the larger Sn^{IV} to reside in six-fold rather than four-fold coordination (the latter being desired for LSnPS) is reflected by the presence of side phases with edge-sharing SnS_6 building units (such as Li_2SnS_3) when stoichiometric amounts of the starting materials are used. A 10–20% excess of Li_2S, however, completely prevents the formation of these layered side phases. It should be noted that we used a slight excess of S yielding approx. 1 atm S at the reaction conditions in order to ensure complete oxidation of Sn and P.

The preparation of phase-pure hypothetical tetragonal $Li_{10}SiP_2S_{12}$ was not successful by means of a conventional solid-state approach. Instead, the main phase at all temperatures between 573 K and 1023 K was the orthorhombic modification of the LSiPS solid solution, which was known to possess distinctly less favorable transport properties.[7] The fact that the tetragonal modification has a slightly higher density than the orthorhombic one (for LGPS, compare ref. 1 and 10), and that a higher Si content should enhance the stability owing to the lower ionic radius of Si led us to the successful preparation of $Li_{11}Si_2PS_{12}$ by high-pressure synthesis (see ESI,† S1 for further details). We obtained almost phase pure $Li_{11}Si_2PS_{12}$, which is referred to as LSiPS in the following.

[a] *Max Planck Institute for Solid State Research, Heisenbergstr. 1, 70569 Stuttgart, Germany. E-mail: a.kuhn@fkf.mpg.de, b.lotsch@fkf.mpg.de*
[b] *Department of Chemistry, Ludwig-Maximilians-Universität München, Butenandtstr. 5-13, 81377 München, Germany*
[c] *Nanosystems Initiative Munich (NIM) and Center for Nanoscience (CeNS), Schellingstr. 4, 80799 München, Germany*

† Electronic supplementary information (ESI) available: Experimental, Rietveld refinement results, supplementary tables, NMR relaxometry details, impedance spectroscopy details, determination of electronic transference number, SEM-EDX, electrochemical stability. See DOI: 10.1039/c4cp02046d

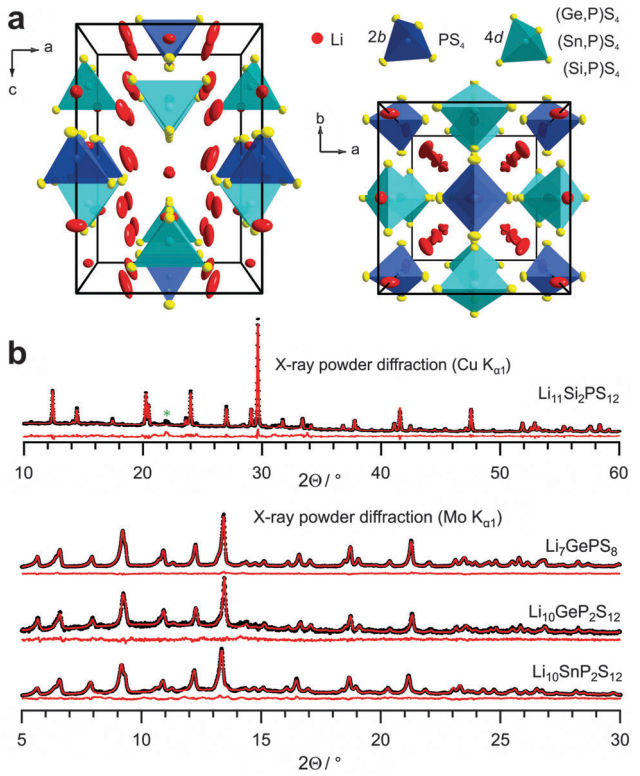

Fig. 1 (a) Crystal structure of tetragonal LGPS as obtained from single-crystal X-ray diffraction.[8] (b) X-ray powder diffraction and Rietveld refinement of $Li_{11}Si_2PS_{12}$ and $Li_{10}SnP_2S_{12}$ in comparison to previously reported $Li_{10}GeP_2S_{12}$ and Li_7GePS_8.[6] The side phase is marked by a green asterisk.

Fig. 1a depicts the unit cell of the generic tetragonal LGPS structure as obtained from single-crystal X-ray diffraction of $Li_{10}GeP_2S_{12}$.[8] The structure contains PS_4 and GeS_4 tetrahedra which are charge-compensated by Li ions. In the tetragonal LGPS structure type, there exist two sets of tetrahedra with the central atom on a 4*d* and 2*b* site, respectively, with the tetrahedra around the 4*d* site being considerably larger. Consequently, in tetragonal LGPS, the 4*d* site is occupied by both Ge and P, while the smaller 2*b* site is solely occupied by P.[1,8] The occupancy of the mixed occupied 4*d* site (Ge_xP_{1-x}) can be varied in the range of $0.5 \leq x(Ge) \leq 0.75$ with the end members of the accessible range of the solid solution being roughly Li_7GePS_8 and $Li_{10}GeP_2S_{12}$.[6,9] Fig. 1b shows the XRD patterns with single-phase Rietveld refinements for $Li_{10}SnP_2S_{12}$ and $Li_{11}Si_2PS_{12}$ in comparison with the patterns for tetragonal LGPS (Li_7GePS_8 and $Li_{10}GeP_2S_{12}$). All samples show the desired tetragonal structure[1,6,8] and are phase-pure on the XRD level except for a weak additional reflection for LSiPS (marked by an asterisk and tentatively ascribed to a high-pressure modification of S[11]). The cell parameters are listed in Table S1 (ESI†). According to the Rietveld refinement (see ESI,† S2), in $Li_{10}SnP_2S_{12}$ the 4*d* site is occupied by Sn and P ($x(Sn) = 0.47$), whereas again, the 2*b* site is occupied by P only. This is in line with the results from single-crystal X-ray diffraction recently published by Bron *et al.*[4] The accessible range of the LSnPS solid solution is much narrower than in case of LGPS – we obtained the tetragonal modification only for values of $x(Sn)$ very close to 0.5. For other Sn/P ratios, two phases were obtained: tetragonal LSnPS of the composition $Li_{10}SnP_2S_{12}$ and the orthorhombic modification as side phase. This can be explained by the larger ionic radius of Sn^{IV} as compared to Ge^{IV}, rendering a higher occupancy of this position relative to P^V energetically unfavourable. The opposite is true for LSiPS: Si^{IV} is only slightly larger than the isoelectronic P^V ion. Therefore, in order to stabilize the tetragonal modification with two sets of differently-sized tetrahedra, the 4*d* site has to be occupied by Si to a much higher extent as compared to Ge or Sn. This explains why the tetragonal modification is obtained for the stoichiometry $Li_{11}Si_2PS_{12}$ rather than $Li_{10}SiP_2S_{12}$.

^{31}P MAS NMR was used in order to probe the relative amount of P residing on the 4*d* and 2*b* sites (*cf.* Fig. 1a). This is of special importance for the structural elucidation of the LSiPS sample because here, this information is not accessible from X-ray diffraction since Si^{IV} and P^V are isoelectronic. Fig. 2 shows the ^{31}P MAS NMR spectra of the tetragonal LGPS-type electrolytes. The spectrum of $Li_{10}SnP_2S_{12}$ is very similar to that of $Li_{10}GeP_2S_{12}$: as expected from Rietveld refinement, the relative intensity of the signals assigned to the 4*d* and 2*b* sites is 1 : 1 within 5% error. The third signal shows the chemical shift typical of the orthorhombic modification, which is, however, not observed in the X-ray patterns. Therefore, we assign it to the presence of a side phase of low crystallinity, which resembles the local structure of the orthorhombic modification (see also ref. 6). For $Li_{11}Si_2PS_{12}$, the structural model assumed above – judging only from the stoichiometry of the sample – is largely verified. Only a small amount of P resides on the mixed-occupied 4*d* site (~10%). Thus, the occupancy of the 4*d* site for all LGPS-type samples follows a clear trend. For the largest ion, Sn, the occupancy is close to $x(Sn) \approx 0.50$. For Ge, the occupancy ranges from $0.5 < x(Ge) < 0.75$, while for the small Si, $x(Si) \approx 0.95$.

In order to characterize the Li diffusivity in the LGPS-type materials $Li_{10}SnP_2S_{12}$ and $Li_{11}Si_2PS_{12}$, we performed ^7Li PFG

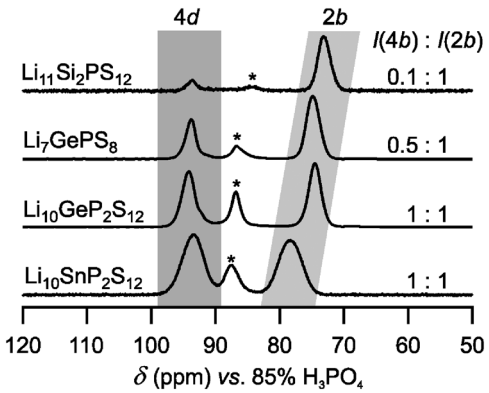

Fig. 2 ^{31}P MAS NMR spectra (ν_{rot} = 12 kHz, B_0 = 9.4 T) of the different isostructural materials crystallizing in the tetragonal LGPS-type. The spectra for Li_7GePS_8 and $Li_{10}GeP_2S_{12}$ as well as the assignment of the lines were taken from ref. 6. The asterisks denote impurities with a chemical shift typical of the orthorhombic modification.

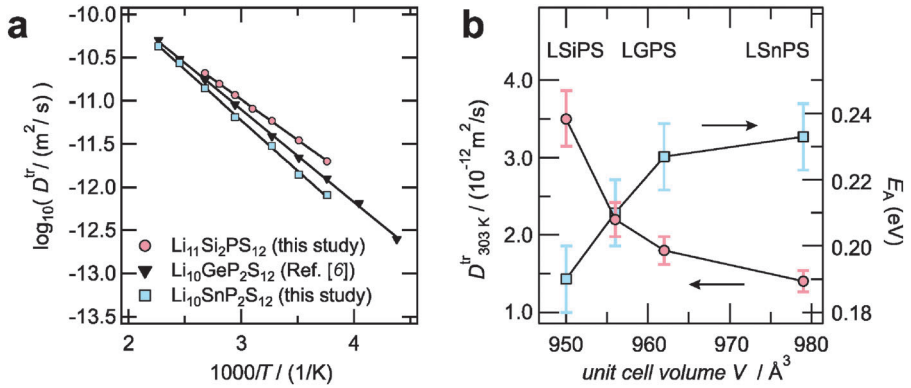

Fig. 3 (a) Li tracer-diffusion coefficients of LGPS-type electrolytes as measured by ^{7}Li PFG NMR. (b) Correlation between diffusion parameters and unit cell volume for LGPS-type electrolytes.

NMR measurements. The obtained Li tracer-diffusion coefficients D^{tr} (3D diffusion, *cf.* ref. 6) are shown in Fig. 3a in comparison with those previously reported for $Li_{10}GeP_2S_{12}$.[6] Note that in all cases, the measured diffusion coefficients can clearly be assigned to diffusion in the bulk of the tetragonal LGPS-type electrolytes, since the quadrupolar structure of the decaying NMR signal showed the finger-print (see Fig. 4a and b) of the tetragonal modification, which is distinct from that of orthorhombic or amorphous side phases. The diffusivity of $Li_{10}SnP_2S_{12}$ is slightly lower than that of $Li_{10}GeP_2S_{12}$ and the activation energy is slightly higher (0.23(1) eV *vs.* 0.21(1) eV). In contrast, the diffusivity of $Li_{11}Si_2PS_{12}$ is even higher than that of $Li_{10}GeP_2S_{12}$ with a slightly lower activation energy (0.19(1) eV *vs.* 0.21(1) eV). We would like to point out that this trend is – both qualitatively and quantitatively – in very good agreement with theoretical calculations by Ong *et al.*[3] as presented in Table 1. Note that the theoretical diffusion coefficients taken from the MD simulation in ref. 3 have been extrapolated from 600 K down to room temperature in order to compare them with our experimental data. As shown in Fig. 3b, a clear correlation between the unit

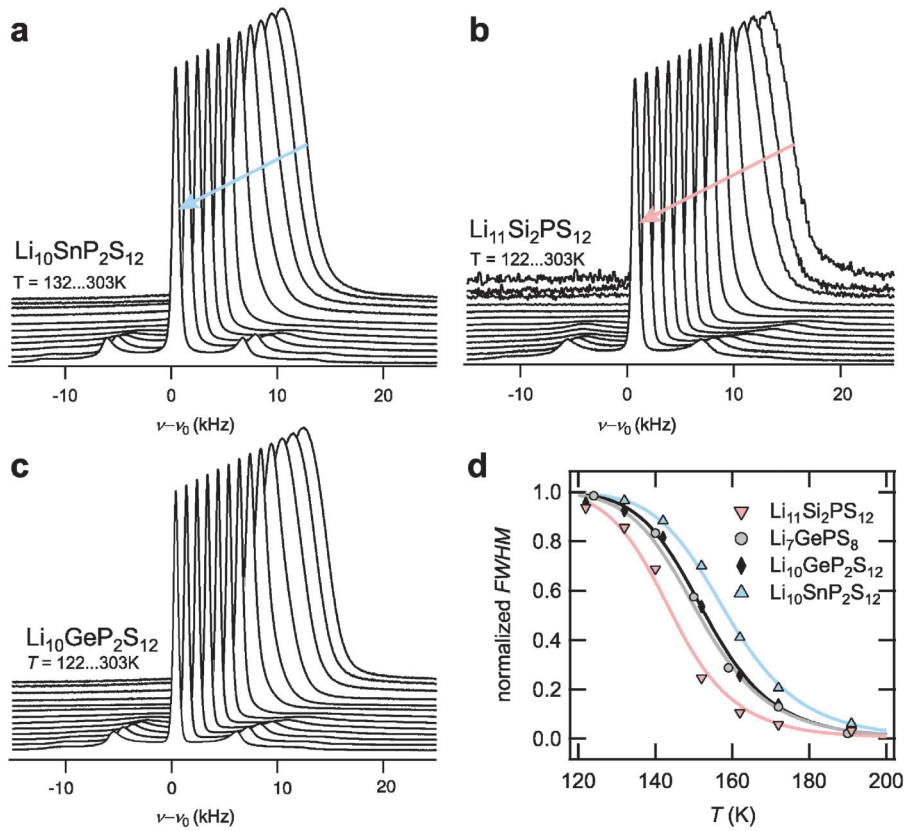

Fig. 4 Temperature-dependent ^{7}Li NMR spectra of (a) $Li_{10}SnP_2S_{12}$, (b) $Li_{11}Si_2PS_{12}$, and (c) $Li_{10}GeP_2S_{12}$ (taken from ref. 6). (d) Comparison of the normalized narrowing curves of the LGPS-type electrolytes.

Table 1 Experimental Li^+ diffusion coefficients at room temperature and activation energies for tetragonal LGPS-type materials obtained from ^{7}Li PFG NMR measurements in comparison with the theoretical ones obtained from MD simulations in ref. 3

Compound	D_{th}[c]/m^2 s^{-1}	D_{exp}/m^2 s^{-1}	$E_{A,th}$/eV	$E_{A,exp}$/eV
$Li_{11}Si_2PS_{12}$	—	3.5×10^{-12} [a]	—	0.19(1) [a]
$Li_{10}SiP_2S_{12}$	1.9×10^{-11} [c]	—	0.20 [d]	—
$Li_{10}GeP_2S_{12}$	1.0×10^{-11} [c]	2.2×10^{-12} [b]	0.22 [d]	0.21(1) [b]
Li_7GePS_8	—	1.8×10^{-12} [b]	—	0.23(1) [b]
$Li_{10}SnP_2S_{12}$	4.4×10^{-12} [c]	1.4×10^{-12} [a]	0.24 [d]	0.23(1) [a]
$Li_{10}SnP_2S_{12}$	—	1.8×10^{-12} [e]	—	—

[a] This work. [b] From ref. 6. [c] Extrapolated from Fig. 3 in ref. 3. [d] From ref. 3. [e] From ref. 4.

cell volume of the tetragonal LGPS-type materials and their diffusion parameters is observed. LSiPS shows the smallest unit cell volume and enhanced Li diffusivity, while LSnPS shows the largest unit cell volume and the lowest diffusivity.

While ^{7}Li PFG NMR probes Li ion dynamics occurring on the micron scale and in the time scale of milliseconds, NMR relaxometry is sensitive to Li site-to-site hopping on the Ångström scale and in the time scale of microseconds (transversal relaxation) or nanoseconds (longitudinal relaxation).[12] Thus, NMR relaxometry allows connecting the observed diffusion processes with their microscopic origin, *i.e.* site-to-site hopping of Li ions in the structure. Here, we measured the transversal relaxation – its Fourier transform being the static ^{7}Li NMR spectrum – in order to probe the Li hopping processes. The temperature-dependent ^{7}Li NMR spectra of LSnPS and LSiPS are displayed in Fig. 4a and b, respectively. As expected for isostructural compounds, the overall behavior of the line shape is very similar to that observed for LGPS[6] (see Fig. 4c). At low temperatures, the central transition of the ^{7}Li line is broad and Gaussian-shaped representing the static homonuclear and heteronuclear dipolar interaction of the ^{7}Li spins with their environment. At higher temperatures, as the Li jump rate exceeds the time scale of the dipolar interactions determined by the rigid-lattice line width, the line narrows successively showing a sharp Lorentzian-shaped line at higher temperatures. From the onset of the motional narrowing at T_{MN}, a jump rate can be assessed according to the narrowing condition $\tau^{-1} \approx \sqrt{M_{2\,\text{rigid lattice}}}$ whereby $M_{2\,\text{rigid lattice}}$ is the second moment of the rigid lattice line.[12] In Fig. 4d, the narrowing curves of the four LGPS-type electrolytes are compared. The trend already observed in PFG NMR is clearly reproduced. The Li jump rates at T_{MN} amount to 1.5×10^4 s^{-1} @ 125 K for LSiPS, 1.4×10^4 s^{-1} @ 135 K for LGPS, and 1.4×10^4 s^{-1} @ 145 K for LSnPS, respectively (values included in Fig. 5d, see ESI,† S4 for further details). As already discussed for the LGPS samples in ref. 6, the distinct quadrupolar powder pattern, which is observed for both LSiPS and LSnPS at higher temperatures, represents the quadrupolar coupling between the quadrupolar moment of the ^{7}Li spins and a mean electric field gradient they are exposed to while diffusing through the tetragonal lattice. As observed in the experiment, this mean electric field gradient retains the axial symmetry of the tetragonal structure (δ_Q = 23.5. . .25.9 kHz, η_Q = 0).

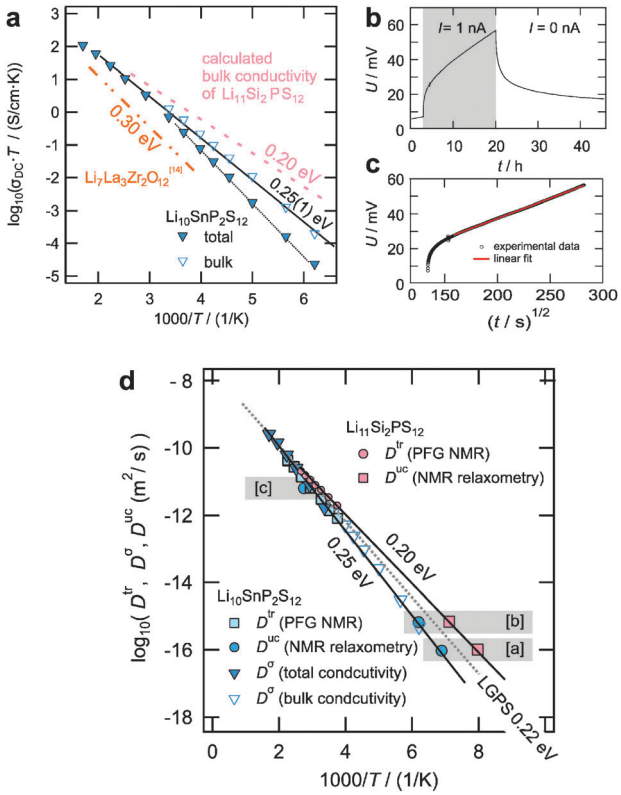

Fig. 5 (a) Total and bulk conductivity of LSnPS as extracted from impedance spectroscopy measurements (see ESI,† for details). The expected bulk conductivity of LSiPS as calculated from NMR diffusivity data is included as a dotted line. For comparison, the dashed dotted line represents the conductivity of the best oxidic solid electrolyte, $Li_7La_3Zr_2O_{12}$. (b) Galvanostatic dc polarization measurement on a symmetric Au|LSnPS|Au cell at 473 K. (c) The polarization curve from (b), as a function of $t^{1/2}$, with linear fit. See text and ESI,† for further details. (d) Comparison of the diffusion coefficients obtained from long-range sensitive methods (PFG NMR, impedance spectroscopy) and short-range sensitive methods (NMR relaxometry) for LSnPS and LSiPS. The data derived from NMR relaxometry stem from [a] motional narrowing of the ^{7}Li central transition (see ESI,† S4), [b] motional averaging of the quadrupolar interaction, (see ESI,† S4), and [c] longitudinal relaxation (see ESI,† S4). The Arrhenius line obtained for LGPS[6] is included as well for comparison.

Thus, the appearance of this distinct quadrupolar powder pattern indicates that the fast Li dynamics measured in fact occurs within crystallites of tetragonal LSnPS or LSiPS.

Impedance spectroscopy was applied in order to study the ionic conductivity of $Li_{10}SnP_2S_{12}$ for which dense ceramic samples could be obtained. Fig. 5a shows the temperature-dependent total conductivity and the bulk conductivity extracted from the impedance spectroscopy measurements for $Li_{10}SnP_2S_{12}$ (see ESI,† for details). The bulk conductivity is activated with 0.25 eV, the room-temperature conductivity amounts to 4 mS cm^{-1}, again in remarkably good agreement with the values predicted from MD simulations[3] (0.24 eV and 6 mS cm^{-1}). For comparison, the bulk conductivity reported by Bron *et al.* for LSnPS was 7 mS cm^{-1}.[4] Table S2 (see ESI,† S3) summarizes the bulk conductivity data for LGPS-type electrolytes as obtained in our measurements. In order to determine

the electronic contribution to the total conductivity, a dc polarization measurement was carried out at 473 K by applying a small current of 1 nA to a symmetric cell with ion blocking Au electrodes Au|LSnPS|Au. Fig. 5b shows the polarization curve. For a good solid electrolyte with vanishingly small electronic contribution one not only expects a considerable polarization but also a small chemical diffusion coefficient. Accordingly, a steady state could not be attained within reasonable waiting time, but an upper limit of the electronic conductivity corresponding to an electronic transference number of $t_{EON} <$ 1 PPM could be safely determined from the absolute voltage values as well as from the time behaviour[13] (linear fit in Fig. 5c, *cf.* ESI,† S5). Thus, LSnPS can be considered as a purely ionic conductor. The impedance of the pellet prior to and after the dc polarization measurement was equal within 1%. For LSiPS, owing to the instability at sintering temperatures, the preparation of phase pure dense ceramic samples suitable for precise impedance spectroscopic experiments failed and we hence concentrate on the NMR results.

Fig. 5d summarizes the results obtained from PFG NMR, NMR relaxometry, and conductivity measurements for LSiPS and LSnPS. For comparison, the jump rates τ^{-1} and the conductivities σ_{dc} were appropriately transformed into diffusion coefficients D^{uc} (uncorrelated diffusion coefficient) and D^{σ} (conductivity diffusion coefficient) using the Einstein–Smoluchowski relation $D^{uc} = a^2/6 \times \tau^{-1}$(jump distance a) and the Nernst–Einstein relation $D^{\sigma} = k_B T/(Nq^2) \times \sigma_{dc}$ (number density of Li^+ N, charge of Li^+ q, Boltzmann's constant k_B). For the calculation, N and an average jump distance of $a \sim 2$Å were deduced from the structure. Obviously, for both $Li_{10}SnP_2S_{12}$ and $Li_{11}Si_2PS_{12}$ the macroscopically observed tracer diffusion can be traced back to 3D Li hopping in the bulk lattice with activation energies of 0.25(1) eV and 0.20(1) eV, respectively. The correlation factor f and the Haven ratio H_R connecting D^{uc} and D^{σ} with D^{tr} *via* $D^{tr} = f \times D^{uc} = H_R \times D^{\sigma}$ are on the order of unity as expected for simple diffusion mechanisms. In view of the very good agreement between the results obtained from NMR techniques and impedance spectroscopy in the case of LGPS and LSnPS, we have calculated the expected bulk conductivity of LSiPS from the Arrhenius line obtained from NMR data (Fig. 5d) using the Nernst–Einstein relation and included it in Fig. 5a. For comparison with other non-LGPS-type electrolytes, the conductivity of the best oxidic solid electrolyte reported to date, $Li_7La_3Zr_2O_{12}$, is included as well.[14] For further comparison, $Li_7La_3Zr_2O_{12}$ shows a conductivity which is almost identical with that of the well-known superionic conductor Li_3N, but significantly lower than that of the LGPS-type electrolytes reported in this study.[15]

Conclusions

The transport properties of $Li_{11}Si_2PS_{12}$, the new tetragonal Si-analogue of the ultrafast electrolyte $Li_{10}GeP_2S_{12}$ are reported, which was obtained under high-pressure conditions for the first time and shown to exhibit the highest room temperature conductivity of any Li solid electrolyte known to date. The structure and Li ion dynamics were characterized in comparison with the Ge-containing parent compound and the Sn analogue, which was comprehensively characterized as well. The Li ion dynamics were elucidated by both long-range sensitive and short-range sensitive techniques and the long-range transport was traced back to Li hopping in the crystalline lattice. In agreement with theoretical predictions, the diffusivity of the Si-compound exceeds that of the Ge-compound while the Sn-analogue shows a lower diffusivity. A clear correlation between the unit cell volume and the diffusivity was observed. Studies of how far the LMePS family is applicable for specific problems of energy research is primarily a question of mechanical stability (*e.g.* sinterability) and chemical stability of specific contacts. Such studies are currently underway, but out of scope of this report. In summary, the observed high ionic conductivity and earth-abundance of its constituents renders the Ge-free LGPS-type electrolyte $Li_{11}Si_2PS_{12}$ a promising candidate for the development of a new generation of all-solid-state batteries.

Acknowledgements

Financial support was granted by the Max Planck Society, the University of Munich (LMU), the Center for NanoScience (CeNS), and the Deutsche Forschungsgemeinschaft (DFG) through the Cluster of Excellence "Nanosystems Initiative Munich" (NIM). B. V. L. gratefully acknowledges financial support by the Fonds der Chemischen Industrie. We thank K. Schunke and U. Engelhardt for help with the high-pressure experiments.

Notes and references

1 N. Kayama, K. Homma, Y. Yamakawa, R. Kanno, M. Yonemura, T. Kamiyama, Y. Kato, S. Hama, K. Kawamoto and A. Mitsui, *Nat. Mater.*, 2011, **10**, 682.
2 Theoretical studies on $Li_{10}GeP_2S_{12}$: (*a*) S. Adams and R. P. Rao, *J. Mater. Chem.*, 2012, **22**, 7687; (*b*) Y. Mo, S. P. Ong and G. Ceder, *Chem. Mater.*, 2012, **24**, 15.
3 S. P. Ong, Y. Mo, W. D. Richards, L. Miara, H. S. Lee and G. Ceder, *Energy Environ. Sci.*, 2013, **6**, 148.
4 P. Bron, S. Johansson, K. Zick, J. Schmedt a. d. Günne, S. Dehnen and B. Roling, *J. Am. Chem. Soc.*, 2013, **135**, 15694.
5 Preliminary results of us on LSnPS and LSiPS had been reported on the occasion of the *112th Bunsentagung*, Karlsruhe, Germany (May 10th 2013), as well as at the *19th International Conference on Solid State Ionics*, Kyoto, Japan (June 3rd 2013).
6 A. Kuhn, V. Duppel and B. V. Lotsch, *Energy Environ. Sci.*, 2013, **6**, 3548.
7 M. Murayama, R. Kanno, M. Irie, S. Ito, T. Hata, N. Sonoyama and Y. Kawamoto, *J. Solid State Chem.*, 2002, **168**, 140.
8 A. Kuhn, J. Köhler and B. V. Lotsch, *Phys. Chem. Chem. Phys.*, 2013, **15**, 11620.

9 R. Kanno, *19th International Conference on Solid State Ionics*, Kyoto, 2013.
10 R. Kanno and M. Murayama, *J. Electrochem. Soc.*, 2001, **148**, A742.
11 M. D. Lind and S. Geller, *J. Chem. Phys.*, 1969, **51**, 348.
12 N. Bloembergen, E. M. Purcell and R. V. Pound, *Phys. Rev.*, 1948, **73**, 679.
13 J. Maier, in *Modern Aspects of Electrochemistry*, ed. C. Vayenas, R. E. White and M. E. Gamboa-Aldeco, Springer, 2007, vol. 41, p. 95.
14 R. Murugan, V. Thangadurai and W. Weppner, *Angew. Chem., Int. Ed.*, 2007, **46**, 7778.
15 A. Rabenau, *Solid State Ionics*, 1982, **6**, 277.